• Basic Research •

Differentially expressed genes in rabbits with traumatic proliferative vitreoretinopathy based on high-throughput sequencing

Yu-Jie Tang[1,2], *Jiang-Ying Liu*[3,4,5,6], *Sheng-Xiang Zhang*[3,4,5,6], *Bo-Yu Liu*[1,2], *Liao Quan*[3,4,5,6], *Qi-Hua Xu*[1,2,6]

[1]The Affiliated Eye Hospital, Jiangxi Medical College, Nanchang University, Nanchang 330006, Jiangxi Province, China
[2]Jiangxi Clinical Research Center for Ophthalmic Disease, Nanchang 330006, Jiangxi Province, China
[3]School of Optometry, Jiangxi Medical College, Nanchang University, Nanchang 330006, Jiangxi Province, China
[4]Jiangxi Research Institute of Ophthalmology and Visual Science, Nanchang 330006, Jiangxi Province, China
[5]Jiangxi Provincial Key Laboratory for Ophthalmology, Nanchang 330006, Jiangxi Province, China
[6]National Clinical Research Center for Ocular Diseases Jiangxi Province Division, Nanchang 330006, Jiangxi Province, China
Co-first Authors: Yu-Jie Tang and Jiang-Ying Liu
Correspondence to: Qi-Hua Xu. The Affiliated Eye Hospital, Jiangxi Medical College, Nanchang University, No.463 Bayi Avenue, Nanchang 330006, Jiangxi Province, China. eye281016@163.com; xu7ganggang@163.com
Received: 2025-04-22 Accepted: 2026-01-16

Abstract

● **AIM:** To identify differentially expressed genes (DEGs) in rabbits with traumatic proliferative vitreoretinopathy (PVR) using high-throughput sequencing (HTS).

● **METHODS:** Thirty-six rabbits were randomly allocated to the control group and the PVR group induced by scleral puncture. On the 28th day following modeling, fundus B-ultrasound and fundus photography were performed on all rabbits, and hematoxylin-eosin (HE) staining was conducted on retinal tissues. RNA sequencing (RNA-Seq) combined with bioinformatics analysis was used to screen PVR-associated DEGs. Gene Ontology (GO) functional enrichment analysis and Kyoto Encyclopedia of Genes and Genomes (KEGG) pathway enrichment analysis were carried out for the identified DEGs. S100A6, EDNRB and CEBPD were randomly selected for quantitative reverse transcription polymerase chain reaction (RT-qPCR) validation to verify the reliability of the RNA-Seq results.

● **RESULTS:** Fundus B-ultrasound, fundus photography and retinal HE staining confirmed the successful establishment of the traumatic PVR rabbit model. A total of 1587 DEGs were screened, of which 1094 were significantly up-regulated and 493 were significantly down-regulated. GO function enrichment analysis showed that these DEGs were mainly enriched in immune response, extracellular region and inflammatory response. KEGG pathway enrichment analysis showed that DEGs were mainly involved in the cytokine-cytokine receptor interaction and hematopoietic cell lineage pathway. RT-qPCR results showed that S100A6, CEBPD and EDNRB were significantly increased in PVR group.

● **CONCLUSION:** A large number of genes exhibit significant differential expression in rabbits with traumatic PVR, among which S100A6, CEBPD and EDNRB may play an important role in traumatic PVR.

● **KEYWORDS:** proliferative vitreoretinopathy; high-throughput sequencing; differentially expressed genes; rabbits

DOI:10.18240/ijo.2026.04.04

Citation: Tang YJ, Liu JY, Zhang SX, Liu BY, Quan L, Xu QH. Differentially expressed genes in rabbits with traumatic proliferative vitreoretinopathy based on high-throughput sequencing. *Int J Ophthalmol* 2026;19(4):665-672

INTRODUCTION

Traumatic proliferative vitreoretinopathy (PVR) is a severe, vision-threatening complication of ocular trauma, occurring in more than 70% of patients with open ocular trauma involving the posterior segment[1]. Pathologically, it is characterized by the growth and contraction of intraocular proliferative membranes, which ultimately lead to traction retinal detachment[2]. Compared to other PVR subtypes, traumatic PVR exhibits a more intense inflammatory response[3]. The occurrence and development of traumatic PVR is multi-factorial, in which the epithelial-mesenchymal

transition (EMT) of retinal pigment epithelial (RPE) cells is the core process[4]. Scarring is the final stage of wound healing. Despite its clinical significance, the lack of in-depth understanding of traumatic PVR pathogenesis has hindered effective treatment development: surgery remains the first-line treatment, but anatomical retinal reattachment rates range only from 43% to 69%[5-6], and severe cases (*e.g.*, funnel-shaped retinal detachment) frequently fail due to persistent tissue hyperplasia exacerbating traction[7-8]. These limitations underscore an urgent need to unravel the molecular mechanisms driving traumatic PVR to identify novel therapeutic targets.

To address this gap, exploring genetic-level mechanisms has emerged as a promising direction. High-throughput sequencing (HTS) technology, a core tool for profiling gene expression, enables comprehensive and rapid detection of global mRNA transcription levels in samples, providing a powerful means to identify key differentially expressed genes (DEGs) and unravel disease mechanisms[9-10]. In PVR research, single-cell RNA sequencing (scRNA-seq) has provided insights into cellular heterogeneity (*e.g.*, abnormally activated immune cells or RPE cells)[4,11], but it focuses on single-cell transcriptional features, potentially overlooking overall tissue level expression trends and carrying risks of bias from cell isolation artifacts or stochastic transcriptional fluctuations. In contrast, tissue-level HTS (bulk RNA-seq) sequences mixed RNA from entire tissue samples, reflecting the average mRNA expression levels across all cell types (including RPE cells, inflammatory cells, and fibroblasts) within the pathological microenvironment. This approach minimizes scRNA-seq-associated artifacts, offers simplified operation, strong sample compatibility, and high data stability-making it ideal for systematically screening key genes and pathways driving PVR pathogenesis.

Here, we employed HTS combined with bioinformatics analysis technology to obtain the DEGs associated with traumatic PVR. By systematically characterizing these molecular signatures, we aim to provide novel insights into traumatic PVR pathogenesis and lay a foundation for developing targeted prevention and treatment strategies.

MATERIALS AND METHODS

Ethical Approval This study has been approved by the Medical Research Ethics Committee of the Affiliated Eye Hospital of Nanchang University, and the approval number is YLP20221206. All procedures involved followed the National Research Council's Guide for the Care and Use of Laboratory Animals.

Animals A total of 36 healthy female adult chinchilla rabbits, weighing 2-2.5 kg and aged 10wk, were purchased from Ganzhou Institute of Animal Husbandry and Fisheries [Ganzhou, Jiangxi Province, China; SCXK(Gan)2018-0009]. All rabbits were kept in an animal house with a temperature of 10℃-25℃ and a humidity of 40%-60%. Eye diseases were eliminated by direct ophthalmoscopy before the experiment. All rabbits used the right eye as the experimental eye.

Main Experimental Instruments and Consumables Slit lamp (Shanghai NIDke Medical Equipment Trading Co., LTD., China), Direct ophthalmoscope (Suzhou Liuliu Vision Technology Co., LTD., China), fundus camera (Chongqing Shangbang Medical Equipment Co., LTD., China), eye B-ultrasound machine (Meda Medical Technology Co., LTD., China), Agelent 2100 Bioanalyzer (Agilent, USA), NanoDrop 2000 Ultra-micro ultraviolet spectrophotometer (Thermo Scientific, USA), inverted fluorescence microscope (OLYMPUS, Japan), PCR instrument (ABI, USA), fluorescence quantitative polymerase chain reaction (PCR) instrument (Roche, Switzerland), Illumina sequencer (Illumina, USA), promecaine hydrochloride eye drops (Alcon Co., LTD., Japan), tobramycin dexamethasone eye drops (Alcon Co., LTD., Japan), tobramycin dexamethasone eye cream (Alcon Co., LTD., Japan), Trizol reagent (Nanjing Nuoweizan Biotechnology Co., LTD., China), primer (Cytology), eyeball fixation solution (Solarbio, China), anhydrous ethanol (Xilong Science, China), mRNA reverse transcription kit (Shanghai Yisheng Biotechnology Co., LTD., China), reverse transcription-polymerase chain reaction (RT-PCR) kit (Shanghai Yisheng Biotechnology Co., LTD., China), Hematoxylin-Eosin staining (HE) staining kit (Solarbio, China) and neutral resin (Sewell, China).

Preparation of Platelet-Rich Plasma Arterial blood 20 mL was extracted from rabbit ears with a syringe, and immediately injected into a vacuum collection vessel (containing sodium citrate), and gently shook the collection vessel for 3min to prevent blood coagulation. Centrifuge 1000×g for 15min, carefully absorbed 1/3 of the supernatant and performed platelet count. The operation was repeated for 3 times and plasma with platelet density of (2.2-2.4)×10^8/mL was obtained.

Establishment of Traumatic PVR Model Thirty-six rabbits were randomly divided into the control group and PVR group, with 18 rabbits in each group. After the PVR group was given compound topicamine eye drops to fully dilate the eyes, The rabbits were then given general and local anesthesia, eyelid opening device was used to open the eyes, 5 mm of the corneoscleral margin above the temporal layer, and the bayonet at 15° was pierced vertically to the center of the vitreous body of the rabbit eye, resulting in scleral puncture about 3 mm. Vitreous body 0.3 mL was carefully sucked out with a 1 mL syringe, and 0.3 mL platelet-rich plasma (PRP) was injected into the vitreous cavity. Within 1wk after the operation, tobramycin dexamethasone was applied to the right eye to prevent infection and inflammation, while the rabbit's dietary

wading was closely observed. Previous experiments have suggested that this modeling method can obtain PVR models with similar grades[12].

Fundus observation after modeling On the 28th day after surgery, all rabbits were dilated with compound tropicamide eye drops. When the pupil dilated to about 8 mm, the changes of vitreous body and retina of rabbit's right eye were examined by fundus camera and ocular B-ultrasound machine successively, and the images were recorded in time. The grading of PVR adopts Fastenberg grading standard[13]. Grade 0, vitreous is transparent, and the fundus is normal; grade 1, formation of proliferative strands in the vitreous; grade 2, preretinal membranous structures are visible with focal traction; grade 3, folds are visible in the posterior pole retina, with possible local retinal detachment; grade 4: extensive retinal detachment (involving the medullary ray and around the optic disc); grade 5, total retinal detachment with visible holes.

Retinal HE Staining In order to observe the changes of fundus of rabbits after modeling, all experimental rabbits were euthanized under deep anesthesia on the 28th day after modeling. An eyeball was randomly taken from each of the two groups and placed into the tissue fixation solution for 1d, and the eyeballs were treated in the order of dehydration, transparency, wax immersion, embedding, and section. The sections were dewaxed, hydrated with high to low concentration alcohol, dyed, dehydrated with low to high concentration, and sealed with neutral gum. After standing for one day, the morphology of the sections was observed under a microscope.

High Throughput Sequencing Technology Retinal tissue was removed and placed into an EP tube containing Trizol, homogenized, and then subjected to chloroform extraction, isopropanol precipitation at -80℃, 75% ice ethanol washing, and dissolution in 20 μL RNase-free water. RNA concentration was measured. For cDNA library construction, ribosomal RNA was removed, followed by RNA fragmentation, reverse transcription, purification, and PCR amplification. Gene expression levels were quantified using fragment per million reads (FPK), and DEGs were screened with DESeq2 software (version 1.16.1) using criteria of $|\log_2 \text{fold change}| \geq 1$ and adjusted $P<0.05$. Gene Ontology (GO) and Kyoto Encyclopedia of Genes and Genomes (KEGG) enrichment analyses of DEGs were performed using DAViD software with hypergeometric distribution test, and $P<0.05$ was considered statistically significant.

RT-qPCR Verified the Sequencing Results In order to verify the reliability of HTS, S100A6, CEBPD and EDNRB which expression was up-regulated in sequencing were randomly selected for RT-qPCR verification. The amplification reaction was performed by fluorescent quantitative PCR instrument.

Table 1 Primer sequence of RT-qPCR

Gene name	Sequence of primers	Tm
S100A6	F: AGGGCTGAAGACAGACTG	60°C
	R: ATCTTACAATCACCCACAC	
CEBPD	F: TGAACTGCGAGAGAAGCTAT	60°C
	R: CCTTAGCTGCATCAACAGGA	
EDNRB	F: CTTACCATTGGCCATCACTG	60°C
	R: AAGGCAATTTGCATTCCAC	
GAPDH	F: TCACCATCTTCCAGGAGCGA	60°C
	R: CACAATGCCGAAGTGGTCGT	

RT-qPCR: Quantitative reverse transcription polymerase chain reaction; Tm: Temperature.

Table 2 PVR classification of rabbits on the 28th day after modeling

Group	PVR grade						Average	*P*
	0	1	2	3	4	5		
Control	18	0	0	0	0	0	0	<0.001
PVR	2	3	6	4	3	0	2.17	

PVR: Proliferative vitreoretinopathy.

The reaction conditions were: 94℃ 30s, 94℃ 5s, 60℃ 30s, 45 cycles. The internal parameter was GAPDH. The experiment was repeated three times for each sample, and the expression was calculated according to $2^{-\Delta\Delta CT}$ method[14]. The sequence of primers is shown in Table 1.

Statistical Analysis GraphPad (version 9.0) software was used to analyze the relevant experimental data. The PVR grade was tested by Mann-Whitney *U* test. The measurement data was expressed as mean±standard deviation (SD). The independent sample *t*-test was used for comparison between groups. $P<0.05$ was considered statistically significant.

RESULTS

Vitreous and Retinal Changes On the 28th day after modeling, there was a statistically significant difference in PVR grading between the PVR group and the control group ($P<0.001$), as shown in Table 2. Fundus photography and ocular B-ultrasound images showed that the vitreous cavity and retina of rabbits in the control group were normal, while the PVR group showed turbidity in the vitreous cavity, extensive proliferating film and retinal detachment in front of the retina (Figures 1 and 2).

HE Staining of the Retina On the 28th day after modeling, HE staining results showed that all retinal layers in the control group were arranged neatly without any special features. In the PVR group, all layers of retinal tissue were disordered and retinal edema was observed (Figure 3).

Sequencing Results

Results of sequencing data preprocessing We obtained a total of 81.91 G of effective data, and the distribution of effective data for each sample ranged from 12.25 to 15.91 G, in which Q30 bases were distributed from 92.13% to 92.85%, and the average GC content was 47.92%. The genome alignment

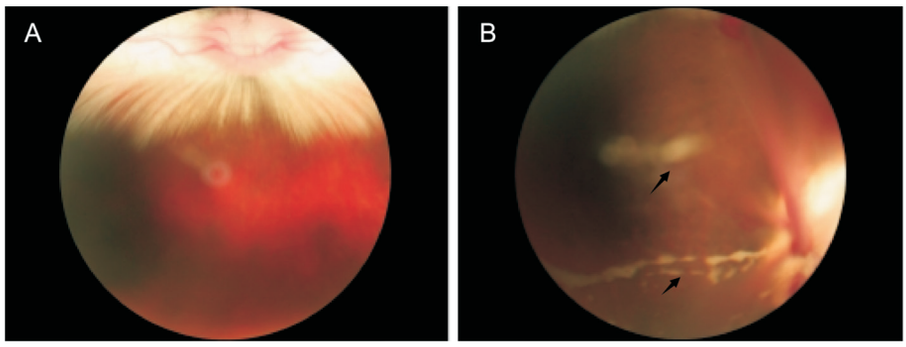

Figure 1 Rabbit fundus image on the 28th day after modeling A: Fundus of rabbit in control group is normal; B: Fundus of rabbit in PVR group: the proliferative membrane on the surface of the retina is clearly visible (black arrow). PVR: Proliferative vitreoretinopathy.

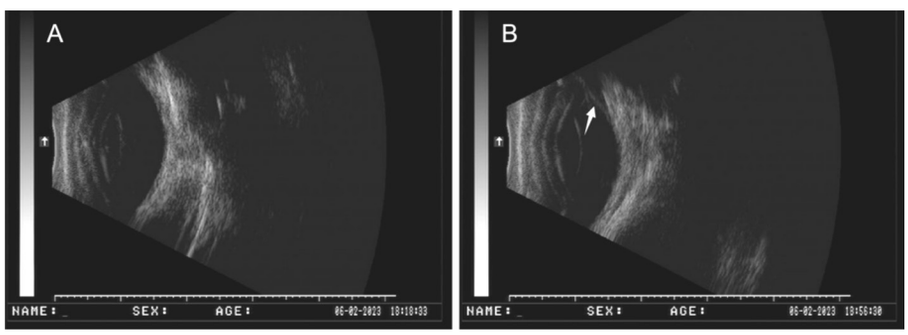

Figure 2 B-ultrasound image on the 28th day after modeling A: B-ultrasound image of rabbit in control group is normal; B: B-ultrasound image of rabbit in PVR group: retinal detachment is obvious (white arrow). PVR: Proliferative vitreoretinopathy.

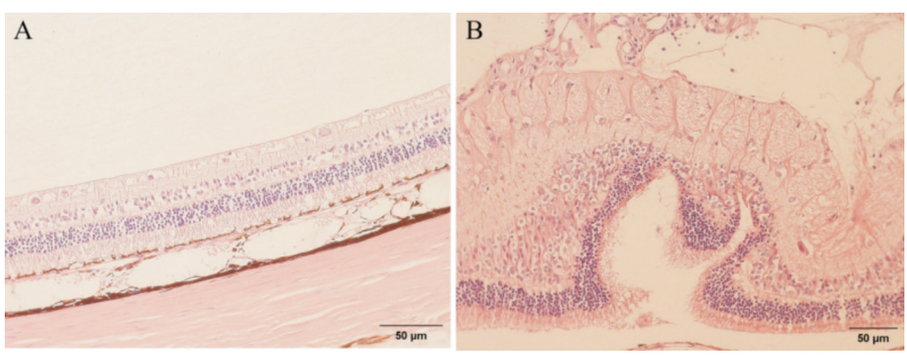

Figure 3 Hematoxylin-Eosin staining of rabbit retina A: Control group, retina layers are arranged neatly; B: PVR group: retina layers are disordered and retinal detachment is clear. Scale bar: 50 μm. PVR: Proliferative vitreoretinopathy.

rates of each sample ranged from 93.62% to 94.34%. The quality preprocessing results of transcriptome sequencing data are shown in Table 3.

Analysis of expression level of DEGs A total of 1587 DEGs were screened, of which 1094 were significantly up-regulated and 493 were significantly down-regulated. The overall distribution of DEGs was shown by volcanic plots respectively, and cluster analysis of DEGs was carried out, as shown in Figure 4A. The results of differential cluster analysis for each group are shown in Figure 4B.

GO and KEGG analysis of DEGs In order to further understand the biological characteristics of DEGs, functional analysis of DEGs was performed using bioinformatics methods. GO enrichment showed that DEGs were enriched in 252 items and mainly concentrated in inflammatory response, immune response, extracellular region and structural constituent of eye lens (Figure 5A). KEGG analysis showed that DEGs are mainly enriched in the cytokine-cytokine receptor interaction pathway and hematopoietic cell lineage pathway (Figure 5B).

Results of RT-qPCR The expression levels of S100A6, CEBPD and EDNRB were increased significantly in the PVR group, and the trend was consistent with the sequencing results (Figure 6).

DISCUSSION

The essence of traumatic PVR is the excessive repair response of eye tissue to traumatic stimuli. How to avoid or mitigate the damage caused by traumatic PVR is a great challenge for clinical ophthalmologists and ophthalmologists. So far, there has been no breakthrough in the treatment of traumatic PVR.

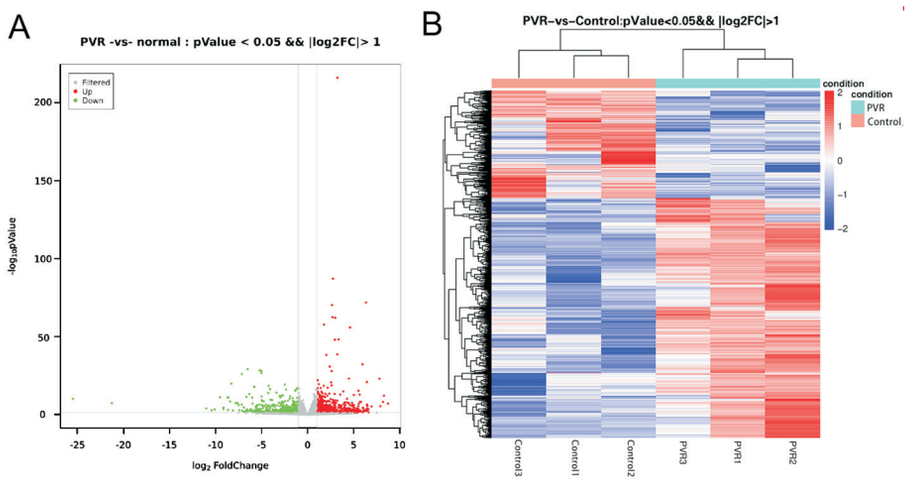

Figure 4 Expression levels of DEGs in the control and PVR groups A: Volcano plot of DEGs, gray is for genes with non-significant differences, red and green are for genes with significant differences in expression; B: Heatmap of DEGs with red representing high-expressed mRNAs and blue representing low-expressed mRNAs. PVR: Proliferative vitreoretinopathy; DEGs: Differentially expressed genes.

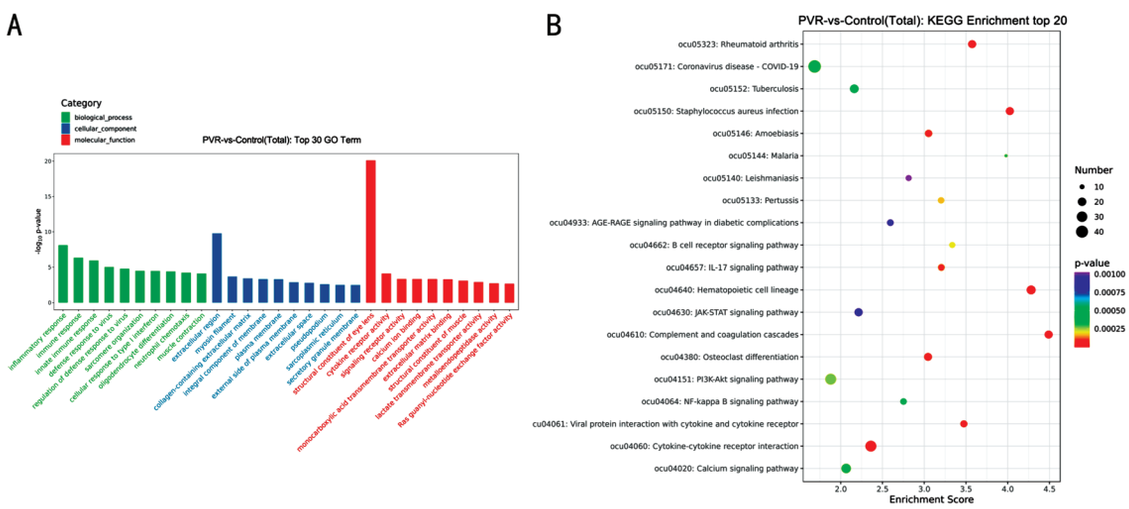

Figure 5 GO and KEGG analysis of DEGs A: Graph of the top 30 enrichment items in the GO enrichment analysis of DEGs; B: KEGG enrichment analysis of DEGs: bubble maps of the top 20 entries. GO: Gene Ontology; KEGG: Kyoto Encyclopedia of Genes and Genomes; DEGs: Differentially expressed genes; PVR: Proliferative vitreoretinopathy.

Table 3 Transcriptome sequencing data preprocessing

Sample	Raw reads	Raw bases	Clean reads	Clean bases	Valid bases	Q30	GC
Control1	87.92 M	13.19 G	86.05 M	12.25 G	92.89%	92.48%	48.95%
Control2	93.14 M	13.97 G	91.15 M	12.97 G	92.84%	92.34%	49.31%
Control3	92.57 M	13.89 G	90.61 M	12.93 G	93.13%	92.36%	48.39%
PVR1	94.48 M	14.17 G	92.41 M	13.12 G	92.60%	92.13%	47.14%
PVR2	115.11 M	17.27 G	112.43 M	15.91 G	92.12%	92.41%	45.79%
PVR3	106.52 M	15.98 G	104.11 M	14.73 G	92.21%	92.85%	47.97%

PVR: Proliferative vitreoretinopathy.

Although vitrectomy is now well developed, studies have shown that the incidence of PVR has not improved.

Due to the complexity of PVR pathogenesis, there has been a lot of research on how to model PVR *in vivo* in the past few decades. Suitable animal models are inevitable in the course of PVR research. In this study, chinchilla rabbit was selected as the experimental object, because it has the advantages of large vitreous body cavity and small lens, which is conducive to reducing the risk of puncture of lens. This advantage is also one of the reasons why rabbits are the best choice for PVR models[15]. The animal modeling methods of PVR are also varied, and the commonly used modeling methods are mainly to inject cells[16-18], blood components[19], cytokines[20-21], and proteases[22] into the vitreous cavity. However, the success rate

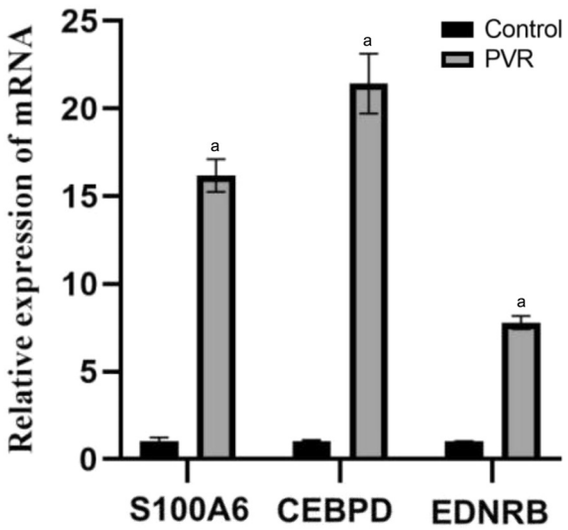

Figure 6 Results of quantitative reverse transcription polymerase chain reaction [a]*P*<0.0001 *vs* control group. PVR: Proliferative vitreoretinopathy.

of the simple injection method is relatively low. In order to improve the success rate of modeling, most scholars adopt the combined method for molding[23]. Our previous studies have suggested that injection of PRP into the vitreous cavity can significantly improve the success rate of modeling on the basis of scleral perforation injury. Since most experimental rabbits developed PVR between 14-28d, we selected the 28th day after modeling as the endpoint for observation.

PVR is a complex fibrotic disorder driven by interactions between RPE cells, fibroblasts, inflammatory cells, and extracellular matrix (ECM) components, mediated by multiple cytokines and signaling pathways. Key cytokines involved in PVR pathogenesis include transforming growth factor-β (TGF-β), platelet-derived growth factor (PDGF), vascular endothelial growth factor (VEGF), interleukin-6 (IL-6), and tumor necrosis factor-α (TNF-α)[24-26]. These cytokines orchestrate pathological processes such as cell proliferation, EMT, ECM deposition, and inflammatory infiltration, which are central to PVR progression. Corresponding signaling pathways activated by these cytokines include the TGF-β/Smad pathway (critical for fibrotic gene transcription), mitogen-activated protein kinase (MAPK) pathway (regulating cell proliferation and migration), phosphatidylinositol 3-kinase (PI3K)/Akt pathway (promoting cell survival), and nuclear factor-κB (NF-κB) pathway (mediating inflammatory responses)[27-29]. For instance, TGF-β ligands bind to transmembrane receptors, phosphorylate Smad2/3, and translocate to the nucleus to induce the expression of fibrotic markers[30].

However, the existing studies on the genetic level of PVR are still not in-depth. In this study, a rabbit model of traumatic PVR was established, and a total of 1587 DEGs were obtained by HTS platform. Through literature review, we found that S100A6 belongs to the S100 family and is a calcium-binding protein involved in the regulation of cytoskeletal assembly and degradation. It has been shown that inhibiting S100A6 expression in rat lung fibroblasts can weaken cell proliferation[31]. This proves that S100A6 is not only related to the cytoskeleton but also promotes cell proliferation. Studies have also shown that S100A6 is involved in cellular oxidative stress[32]. S100A6 is widely expressed in a variety of cancers and is therefore considered as a marker for disease diagnosis and prognosis assessment[33]. Otherwise, tumor cell-secreted S100A6 promotes lymphatic metastasis of liver cancer by upregulating VEGF-D *via* the RAGE/NF-κB/VEGF-D pathway[34]. It can also be used as a marker for stem cells[35-36]. Which means it has the ability to repair damage. These effects are highly consistent with the pathogenesis of PVR. So, we speculate that S100A6 has the potential to be a marker of traumatic PVR, but further experiments are needed to confirm it. As a member of the C/EBP family, CEBPD is normally low in expression, but rapidly increases in response to immune activation and external stimulation[37]. Because it can not only promote the transduction of inflammatory signaling pathways, but also inhibit inflammatory responses, which may be related to the cell state and the environment. CEBPD is a known downstream target of IL-6/STAT3 and TNF-α/NF-κB signaling pathways[38]. At the same time, studies have shown that it is both a tumor suppressor and a tumor promoter[39-40]. Therefore, CEBPD can be used as both a protective factor and a risk factor in the development of the disease. CEBPD is also closely related to fibrotic response. There may be a balance point in between, and the tilt of the balance point determines its positive or negative effects. Finding this balance point will help us further understand the role of CEBPD in traumatic PVR, and hopefully make it play a protective role in traumatic PVR by controlling this balance point. EDNRB is often regarded as a tumor suppressor gene, which is involved in the development of cancers including prostate and breast cancer[41]. Some studies have shown that EDNRB is related to MAPK signaling pathway and promotes cell proliferation and migration[42].

The increasing precision of HTS is expected to advance personalized treatment of traumatic PVR diseases. This sequencing has laid a solid foundation and new insights for further exploration of traumatic PVR related research. Of course, this study has some shortcomings. First of all, it is necessary to further functional verification of the molecular mechanism of these DEGs, and we can obtain the internal correlation between genes through further relevant experiments and bioinformatics methods. Second, *in vitro* sequencing results were lack, and the combination of *in vivo* and *in vitro*

sequencing results is more convincing. Furthermore, we lack multi-time point, single-cell sequencing of traumatic PVR tissue. We know that multiple cells are involved in the development of traumatic PVR, but it is unknown which cells play a decisive role.

In conclusion, numerous genes exhibit significant differential expression in a rabbit model of traumatic proliferative vitreoretinopathy, among which S100A6, CEBPD and EDNRB may serve as potential biomarkers and therapeutic targets.

ACKNOWLEDGEMENTS

Foundations: Supported by the National Natural Science Foundation of China (No.82260210); the Natural Science Foundation of Jiangxi Province (No.20252BAC250122); the Science and Technology Planning Project of Jiangxi Provincial Health Commission (No.202510055); Jiangxi Province Graduate Innovation Special Fund (No.YC2025-B211); Jiangxi Association for Science Education (No.2025KXJYS019).

Conflicts of Interest: Tang YJ, None; **Liu JY,** None; **Zhang SX,** None; **Liu BY,** None; **Quan L,** None; **Xu QH,** None.

REFERENCES

1 Dai J, Zhou X, Bai H, *et al*. Pathogenic mechanisms and treatment advances in proliferative vitreoretinopathy: a review. *Medicine* 2025;104(39):e44804.

2 Idrees S, Sridhar J, Kuriyan AE. Proliferative vitreoretinopathy: a review. *Int Ophthalmol Clin* 2019;59(1):221-240.

3 Stepp MA, Menko AS. Immune responses to injury and their links to eye disease. *Transl Res* 2021;236:52-71.

4 Liao M, Zhu X, Lu Y, *et al*. Multi-omics profiling of retinal pigment epithelium reveals enhancer-driven activation of RANK-NFATc1 signaling in traumatic proliferative vitreoretinopathy. *Nat Commun* 2024;15:7324.

5 Ferro Desideri L, Artemiev D, Zandi S, *et al*. Proliferative vitreoretinopathy: an update on the current and emerging treatment options. *Graefes Arch Clin Exp Ophthalmol* 2024;262(3):679-687.

6 Anguita R, Roth J, Makuloluwa A, *et al*. Late presentation of retinal detachment: clinical features and surgical outcomes. *Retina* 2021;41(9):1833-1838.

7 Assi A, Khoueir Z, Helou C, *et al*. Intraocular application of mitomycin C to prevent proliferative vitreoretinopathy in perforating and severe intraocular foreign body injuries. *Eye* (*Lond*) 2019;33(8):1261-1270.

8 Chen XF, Du M, Wang XH, *et al*. Effect of etanercept on post-traumatic proliferative vitreoretinopathy. *Int J Ophthalmol* 2019;12(5):731-738.

9 Dongare DB, Nishad SS, Mastoli SY, *et al*. High-throughput sequencing: a breakthrough in molecular diagnosis for precision medicine. *Funct Integr Genom* 2025;25(1):22.

10 Smail C, Montgomery SB. RNA sequencing in disease diagnosis. *Annu Rev Genom Hum Genet* 2024;25:353-367.

11 Santiago CP, Gimmen MY, Lu YC, *et al*. Comparative analysis of single-cell and single-nucleus RNA-sequencing in a rabbit model of retinal detachment-related proliferative vitreoretinopathy. *Ophthalmol Sci* 2023;3(4):100335.

12 Chen J, Wu L, Wang Z, *et al*. Establishment of a rabbit model of traumatic proliferative vitreoretinopathy using three methods. *Chinese Journal of Pathophysiology* 2022;38(5):954-960.

13 Yang S, Li H, Yao H, *et al*. Long noncoding RNA ERLR mediates epithelial-mesenchymal transition of retinal pigment epithelial cells and promotes experimental proliferative vitreoretinopathy. *Cell Death Differ* 2021;28(8):2351-2366.

14 Rao X, Huang X, Zhou Z, *et al*. An improvement of the 2ˆ(-delta delta CT) method for quantitative real-time polymerase chain reaction data analysis. *Biostatistics, Bioinformatics and Biomathematics* 2013;3(3):71-85.

15 Agrawal RN, He S, Spee C, *et al*. *In vivo* models of proliferative vitreoretinopathy. *Nat Protoc* 2007;2(1):67-77.

16 Behar-Cohen FF, Thillaye-Goldenberg B, de Bizemont T, *et al*. EIU in the rat promotes the potential of syngeneic retinal cells injected into the vitreous cavity to induce PVR. *Invest Ophthalmol Vis Sci* 2000;41(12):3915-3924.

17 Grierson I, Boulton M, Hiscott P, *et al*. Human retinal pigment epithelial cells in the vitreous of the owl monkey. *Exp Eye Res* 1986;43(4):491-502.

18 Mandelcorn MS, Machemer R, Fineberg E, *et al*. Proliferation and metaplasia of intravitreal retinal pigment epithelium cell autotransplants. *Am J Ophthalmol* 1975;80(2):227-237.

19 Zheng XZ, Du LF, Wang HP. A immunohistochemical analysis of a rat model of proliferative vitreoretinopathy and a comparison of the expression of TGF-β and PDGF among the induction methods. *Bosn J Basic Med Sci* 2010;10(3):204-209.

20 Ishikawa K, He S, Terasaki H, *et al*. Resveratrol inhibits epithelial-mesenchymal transition of retinal pigment epithelium and development of proliferative vitreoretinopathy. *Sci Rep* 2015;5:16386.

21 Pao SI, Lin LT, Chen YH, *et al*. Repression of Smad4 by microRNA-1285 moderates TGF-β-induced epithelial-mesenchymal transition in proliferative vitreoretinopathy. *PLoS One* 2021;16(8):e0254873.

22 Cantó Soler MV, Gallo JE, Dodds RA, *et al*. A mouse model of proliferative vitreoretinopathy induced by dispase. *Exp Eye Res* 2002;75(5):491-504.

23 Khanum BNMK, Guha R, Sur VP, *et al*. Pirfenidone inhibits post-traumatic proliferative vitreoretinopathy. *Eye (Lond)* 2017;31(9):1317-1328.

24 Xiao R, Lei C, Zhang Y, *et al*. Interleukin-6 in retinal diseases: from pathogenesis to therapy. *Exp Eye Res* 2023;233:109556.

25 Gao F, Li M, Zhu L, *et al*. Knockdown of HSPA13 inhibits TGFβ1-induced epithelial-mesenchymal transition of RPE by suppressing the PI3K/Akt signaling pathway. *Invest Ophthalmol Vis Sci* 2024;65(11):1.

26 Duan Y, Wu W, Cui J, *et al*. Ligand-independent activation of platelet-derived growth factor receptor β promotes vitreous-induced contraction of retinal pigment epithelial cells. *BMC Ophthalmol* 2023;23(1):344.

27 Wang V, Heffer A, Roztocil E, *et al*. TNF-α and NF-κB signaling play a critical role in cigarette smoke-induced epithelial-mesenchymal transition of retinal pigment epithelial cells in proliferative vitreoretinopathy. *PLoS One* 2022;17(9):e0271950.

28 Hsiao CC, Chang YC, Hsiao YT, *et al*. Triamcinolone acetonide modulates TGF-β2-induced angiogenic and tissue-remodeling effects in cultured human retinal pigment epithelial cells. *Mol Med Rep* 2021;24(5):802.

29 Huang H, Huang Q, Wang J, *et al*. Hirudo extract ameliorates proliferative vitreoretinopathy by promoting autophagy and attenuating the THBS2/PI3K/Akt pathway. *Sci Rep* 2025;15(1):1287.

30 Ma X, Xie Y, Gong Y, *et al*. Silibinin prevents TGFβ-induced EMT of RPE in proliferative vitreoretinopathy by inhibiting Stat3 and Smad3 phosphorylation. *Invest Ophthalmol Vis Sci* 2023;64(13):47.

31 Wang Y, Kang X, Kang X, *et al*. S100A6: molecular function and biomarker role. *Biomark Res* 2023;11(1):78.

32 Leśniak W, Szczepańska A, Kuźnicki J. Calcyclin (S100A6) expression is stimulated by agents evoking oxidative stress *via* the antioxidant response element. *Biochim Biophys Acta* 2005;1744(1):29-37.

33 Yang F, Ma J, Zhu D, *et al*. The role of S100A6 in human diseases: molecular mechanisms and therapeutic potential. *Biomolecules* 2023;13(7):1139.

34 Chen T, Ruan Y, Ji L, *et al*. S100A6 drives lymphatic metastasis of liver cancer *via* activation of the RAGE/NF-κB/VEGF-D pathway. *Cancer Lett* 2024;587:216709.

35 Chovatiya G, Ghuwalewala S, Walter LD, *et al*. High-resolution single-cell transcriptomics reveals heterogeneity of self-renewing hair follicle stem cells. *Exp Dermatol* 2021;30(4):457-471.

36 Joost S, Zeisel A, Jacob T, *et al*. Single-cell transcriptomics reveals that differentiation and spatial signatures shape epidermal and hair follicle heterogeneity. *Cell Syst* 2016;3(3):221-237.e9.

37 Lai HY, Hsu LW, Tsai HH, *et al*. CCAAT/enhancer-binding protein delta promotes intracellular lipid accumulation in M1 macrophages of vascular lesions. *Cardiovasc Res* 2017;113(11):1376-1388.

38 Sanford DC, DeWille JW. C/EBPδ is a downstream mediator of IL-6 induced growth inhibition of prostate cancer cells. *Prostate* 2005;63(2):143-154.

39 Shanley M, Daher M, Dou J, *et al*. Interleukin-21 engineering enhances NK cell activity against glioblastoma *via* CEBPD. *Cancer Cell* 2024;42(8):1450-1466.e11.

40 Mao XG, Xue XY, Lv R, *et al*. CEBPD is a master transcriptional factor for hypoxia regulated proteins in glioblastoma and augments hypoxia induced invasion through extracellular matrix-integrin mediated EGFR/PI3K pathway. *Cell Death Dis* 2023;14(4):269.

41 Liu S, Zhang J, Zhu J, *et al*. Prognostic values of EDNRB in triple-negative breast cancer. *Oncol Lett* 2020;20(5):1.

42 Miglietta A, Bozzo F, Bocca C, *et al*. Conjugated linoleic acid induces apoptosis in MDA-MB-231 breast cancer cells through ERK/MAPK signalling and mitochondrial pathway. *Cancer Lett* 2006;234(2):149-157.